Hydrodynamics of Gas-Liquid-Solid Annular Fluidization

In a strict sense, operation of the three-phase ebullated bed reactor used in the H-Oil process is not characterized by conventional three-phase fluidization, but by annular three-phase fluidization. In annular three-phase fluidized beds differences in the hydrodynamic behavior over that found in conventional beds occur through changes in the bubble behavior. The addition of a concentrically located inner column in a gas-liquid-solid fluidized bed promotes bubble coalescence. This increase in coalescence can be observed either through changes in the liquid velocity of transition from the coalesced bubble regime to the dispersed bubble flow regime or through changes in holdup behavior. A hydraulic diameter defined for the annulus region proves suitable when comparing different annular systems having the same outside column diameter, but unsuitable when comparing systems having different outside column diameters.

Liang-Shih Fan, Kunihiro Kitano and B. E. Kreischer
Department of Chemical Engineering
Ohio State University
Columbus, OH 43210

Introduction

Gas-liquid-solid fluidized beds provide one important means of conducting three-phase chemical reactions. Several possible industrial applications include processes in the polymer, petrochemical, and biochemical industries (Johnson and Rapp, 1964; Van Driesen and Stewart, 1964; Eccles and De Vax, 1981; Hirata et al., 1982). Two industrial petrochemical processes, the H-Oil process and the L.C. Fining process, employ an ebullated bed three-phase reactor. The ebullated bed reactor applies gas-liquid-solid fluidized bed technology to the hydrocracking, hydrodemetallization, and hydrodesulfurization of heavy residual oils in petroleum processing. Within the reactor, an upward cocurrent flow of oil, hydrogen gas, and product gas supports the bed of catalyst particles. An internal recycle of liquid and entrained gases through a pipe concentrically located within the reactor provides the flow rate required to support the catalyst bed. The magnitude of the recycle rate dictates using a pipe that may be of sufficient size to alter the bed hydrodynamic behavior. In a rigorous treatment the operation of the ebullated bed reactor is not characterized by three-phase fluidization but by annular three-phase fluidization.

The addition of an internal column or pipe within a reactor imposes physical constraints upon the hydrodynamics not experienced in conventional fluidized beds. Ramamurthy and Subbarju (1973) found that for liquid-solid fluidized beds, the inside column had little effect if $D_h/d_p > 8$; where D_h is the hydraulic diameter and d_p is the particle diameter. Dakshinamurty et al. (1972) found that the presence of an inside column slightly altered the bed expansion characteristics. Any effects the annulus size has on the bed hydrodynamics will be closely related to effects of changing the column diameter. Previous studies have presented some information on the effect column diameter has on the bed hydrodynamics. The column diameter affects the transition between flow regimes (Matsuura and Fan, 1984; Fan et al., 1985; Fan et al., 1986). This fact, coupled with Michelsen and Ostergaard's (1970) observation that flow regime strongly affects gas holdup, suggests that gas holdup will also vary with column diameter. The gas holdup and bed expansion correlations of Begovich and Watson (1978) empirically incorporate the effect of column diameter. According to their correlation, both gas holdup and bed expansion will increase with a decrease in column diameter. The column diameter also affects the terminal rise velocity of a bubble. For bubbles of equal size in columns of different sizes, the bubble in the larger column will rise faster (Wallis, 1969). Akita and Yoshida (1974) reported bubble size increases with a decrease in column diameter.

This study examined the hydrodynamic behavior of an annular three-phase fluidized bed. Experiments were conducted to characterize the hydrodynamic behavior over a range of gas and liquid velocities using several different annulus configurations. An analysis of the gas holdup, solids holdup, and flow regime

Correspondence concerning this paper should be addressed to Liang-Shih Fan.

transition data provides a fundamental understanding of annular fluidization.

Experimental

A diagram of the experimental annular fluidized bed is shown in Figure 1. The apparatus consisted of a 15.2 cm ID cast acrylic outside column 122 cm in height. An interchangeable inside column was concentrically located within the outside column. Inside column diameters of 5.1, 8.3, and 11.4 cm were used. Nine pressure taps were located at 15.2 cm intervals along the outside column, with two additional taps located near the distributor at 5.1 cm intervals. A wire mesh retaining grid placed on top of the inside column prevented the loss of particles from the column.

The distributor consisted of three sections: the plenum chamber, the gas-liquid distributor, and a fixed-bed mixer. The gas-liquid distributor allowed liquid to pass from the plenum chamber to the fixed-bed mixer through 6 mm ID acrylic tubes ending in 1.6 mm injection holes. Gas entered the distributor through two ports located on the side walls and exited through 340 injection holes of 1 mm dia.

The experimental conditions used are listed in Table 1. This range of conditions assured experimentation in both the coalesced bubble and dispersed bubble regimes. Both 1 mm and 3 mm glass beads were used to provide distinctively different hydrodynamic behavior. The 1 mm glass beads had a density of 2.87 g/cm^3 and a terminal velocity of 17 cm/s; the 3 mm glass beads had a density of 2.52 g/cm^3 and a terminal velocity of 38 cm/s.

Local gas holdup, mean bubble size, and bubble size distributions were obtained using a twin-electrode conductivity probe developed by Matsuura and Fan (1984). Basically, the probe consisted of two stainless steel syringe needles of 0.2 mm dia. exposed to the local environment. The needles were insulated and maintained apart from each other by epoxy resin. The vertical distance separating the two electrode tips was 0.3 mm. The probe was fixed to a stainless steel tube that acted as the system ground. Further details of the probe construction, signal processing, signal acquisition and matching methods, and signal processing are given by Matsuura and Fan. The bubble velocity was determined from the time elapsed between when a bubble hit the first probe and when it hit the second probe. The bubble chord length was determined from the time elapsed as the bubble passed the probe and the measured bubble velocity.

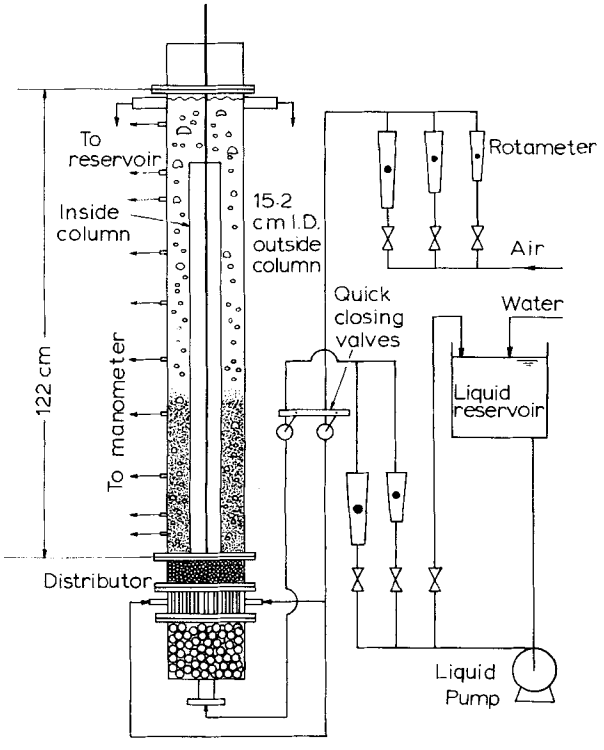

Figure 1. Experimental apparatus.

Table 1. Experimental Conditions

System	d_p mm	U_g cm/s	U_l cm/s	D_i cm
Air-water-glass	3	0–13.1	4.5–9.1	0, 5.1, 8.3, 11.4
Air-water-glass	1	0–9.8	2.5–4.5	0, 5.1, 8.3
Air-water	—	0–13.1	4.5–9.1	0, 5.1, 8.3, 11.4

Conditions at 70°F and ambient pressure.

Results

Flow regime

The hydrodynamic behavior of gas-liquid-solid fluidized beds can be classified into three basic flow regimes on the basis of bubble behavior: the dispersed bubble, coalesced bubble, and slug flow regimes (Muroyama and Fan, 1985). Each of these flow regimes can be identified by its characteristic behavior. The coalesced bubble regime consists of large bubbles having a broad size distribution and a relatively low bed expansion. The dispersed bubble regime consists of small bubbles having a nearly uniform size distribution and a relatively large bed expansion. The slug flow regime consists of bubbles approaching the size of the column itself. Determining the flow regime required identifying these characteristics. One method of identification was by visual observation of the flow behavior and a second was by quantitative measurement of the bubble size distribution.

A flow regime map constructed by visual observation is shown in Figure 2. The map shows the gas and liquid velocities under which the dispersed bubble and coalesced bubble regimes occurred. Two important points are evident in the flow regime map. First, the liquid velocity for regime transition increased as the annulus region became smaller. In the fluidization of 3 mm particles, the transition velocity was 6 cm/s for the nonannular case, while for the three annular systems the transition velocities were 6.9, 8.0, and 9.0 cm/s. Second, both 1 mm and 3 mm particle systems showed similar regime transition behavior despite their overall differences in hydrodynamic behavior.

Analysis of the bubble size distributions also indicated the shift in transition velocity identified on the flow regime map. For example, in 3 mm particle systems the bubble size distributions were determined for each annulus configuration at gas and liquid velocities of 9.4 and 6.9 cm/s, respectively. In each determination the probe was located in the center of the annulus region at two-thirds the expanded bed height. The bubble sizes obtained in the nonannular configuration followed a log normal distribution characteristic of the dispersed bubble flow regime. A typical log normal distribution obtained in the nonannular

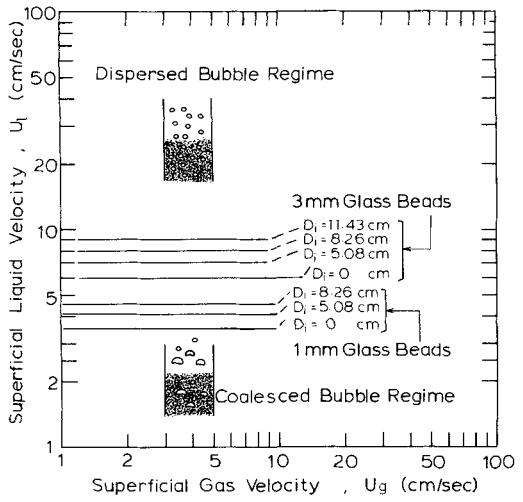

Figure 2. Flow regime map for annular gas-liquid-solid fluidized bed.

configuration is shown in Figure 3. A comparison of bubble size distributions for a nonannular system and annular systems with inside column diameters of 5.1 and 8.3 cm is shown in Figure 4. The comparison indicates that a broadening of the size distribution accompanied the change to an annular fluidized bed. This effect was evident through an increase in mean bubble size from 3.2 mm in the nonannular case to 5.7 mm in the 8.3 cm inside column case. In addition to a larger mean bubble size, the distribution showed bimodal tendencies in the annular systems. Further increasing the inside column diameter to 11.4 cm increased the bimodal aspect of the bubble size distribution; however, the mean bubble size decreased. A comparison of the bubble size distributions for the annular systems with inside column diameters of 11.4 and 8.3 cm is shown in Figure 5. Despite a decrease in the mean bubble diameter when going from the 8.3 cm to the 11.4 cm inside column system, the ratio of the mean bubble diameter to the annulus thickness increased. The larger mean bubble diameter and broader size distributions obtained in the annular fluidized bed over those obtained in a conventional bed indicates that increased bubble coalescence occurs in the annular system.

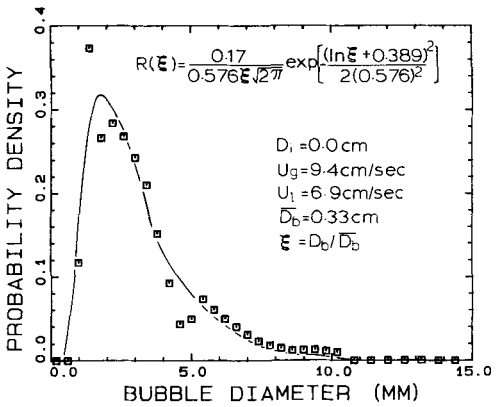

Figure 3. Log normal bubble size distribution for nonannular system.
3 mm glass beads; U_l = 6.9 cm/s; U_g = 9.4 cm/s

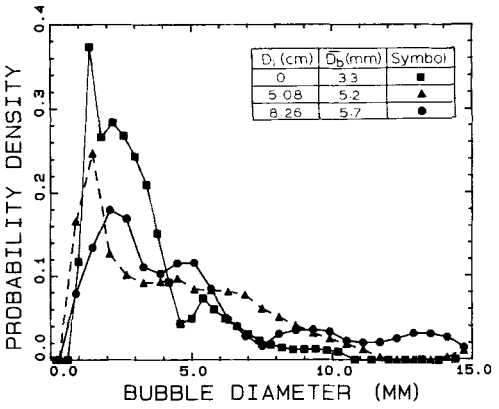

Figure 4. Effect of inside column diameter on bubble size distribution.
3 mm glass beads; U_l = 6.9 cm/s; U_g = 9.4 cm/s

Phase holdups

The overall holdups of the individual phases were determined directly from measurement of the weight of particles within the bed and the static pressure gradient. The following relationships hold for the phase holdups:

$$\epsilon_s = \frac{(W/\rho_s)}{AH} \tag{1}$$

$$-\frac{1}{g}\frac{\Delta P}{\Delta Z} = \epsilon_g\rho_g + \epsilon_l\rho_l + \epsilon_s\rho_s \tag{2}$$

$$1 = \epsilon_g + \epsilon_l + \epsilon_s \tag{3}$$

Local gas holdups were determined using the conductivity probe of Matsuura and Fan (1984).

Bed expansion

The degree of bed expansion as a function of gas velocity depended on the flow regime of the fluidized bed. In the coalesced bubble regime, bed expansion was relatively small, while in the dispersed bubble regime larger bed expansion occurred. The bed expansion behavior for 3 mm particles is shown in Fig-

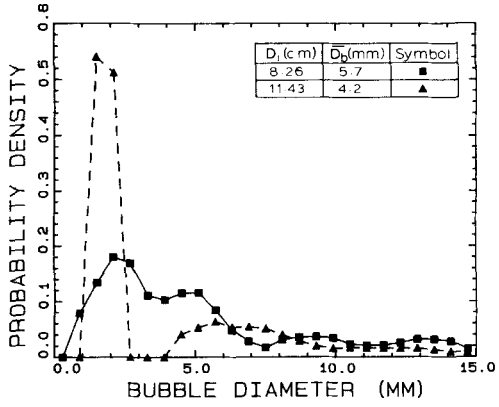

Figure 5. Bubble size distributions in 8.3 and 11.4 cm inside column annular systems.
3 mm glass beads; U_l = 6.9 cm/s; U_g = 9.4 cm/s

ure 6. In the coalesced bubble regime (U_l = 4.5 cm/s), as the gas velocity increased from 2.0 to 12.1 cm/s the bed expanded about 15%. In the dispersed bubble regime (U_l = 9.1 cm/s), over the same range of gas velocities, the bed expanded over 30%. At liquid velocities where the flow regimes were independent of the annulus size, the bed expansion also proved independent of the annulus size. However, at a liquid velocity of 6.9 cm/s, one in which the annulus size clearly affected the flow regime, the annulus size altered the bed expansion behavior in a way consistent with the observed changes in flow regime behavior.

Local gas holdup

Systematically changing the radial location of the conductivity probe produced a qualitative radial profile of the gas holdup. The local gas holdup profiles obtained in the 5.1 cm inside column annulus configuration for both a gas-liquid system and a gas-liquid-3 mm glass bead system are shown in Figure 7. The profiles in the coalesced bubble and dispersed bubble flow regimes differ: in the coalesced bubble regime the profile was parabolic, while in the dispersed bubble regime the profile was essentially flat. The profiles for the gas-liquid and gas-liquid-solid systems show similar behavior; however, for both the coalesced bubble and dispersed bubble regimes the three-phase system showed a larger holdup.

Overall gas holdup

Typical gas holdup data for gas-liquid-solid fluidized beds of 3 mm and 1 mm particles in the dispersed flow regime are shown in Figures 8 and 9. Gas holdup data for a gas-liquid system is shown in Figure 10. In general for the dispersed regime, the 3 mm particle systems yielded larger gas holdup than did the gas-liquid system, while the 1 mm particle systems yielded a lower holdup than the gas-liquid system. The inside column affected the holdup in both the 3 mm particle and gas-liquid systems: in each case the holdup became smaller as the annulus region became smaller. The 1 mm particle systems, however, showed no recognizable trend.

For 3 mm particle systems, the gas holdup data exhibited a wider degree of scatter in the coalesced regime than the dispersed regime, while in 1 mm particle systems the degree of scatter was nearly equal for both regimes. In both cases, the coalesced regime had lower gas holdup than in the dispersed regime. Gas holdup data in the coalesced regime, using 1 mm

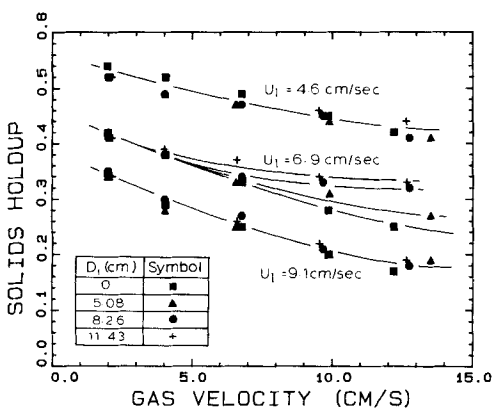

Figure 6. Bed expansion behavior in annular fluidized beds for several liquid velocities.

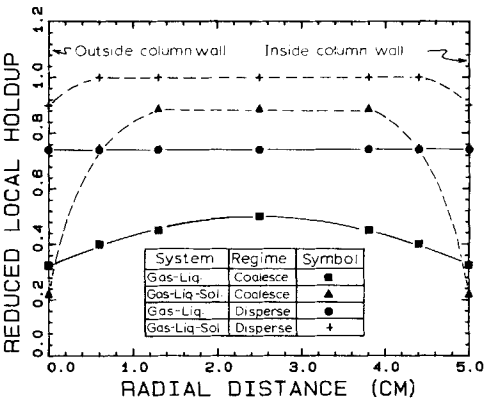

Figure 7. Radial profile of local gas holdup in gas-liquid and gas-liquid-solid annular system.
5.1 cm inside column diameter

particles, is shown in Figure 11; the data show higher gas holdups for smaller annulus sizes. In the coalesced bubble regime using 3 mm particles, however, no such recognizable trend occurred.

Discussion

The experimental results show significant changes in the hydrodynamic behavior of annular systems over conventional systems. The velocity of transition from the coalesced bubble to the dispersed bubble regime increases in all annular systems, the mean bubble size increases in small bubble systems, and gas holdup decreases in small bubble systems. Each of these phenomena is a manifestation of the bubble behavior.

One measure of the bubble behavior is an effective bubble diameter for the system. Akita and Yoshida (1974) found that the effective bubble diameter increased with a decrease in column diameter. Annular systems show similar behavior with respect to a hydraulic diameter. The hydraulic diameter D_h, defined as

$$\frac{D_h}{D_o} = \left(1 - \frac{D_i}{D_o}\right) \tag{4}$$

relates the actual flow area and wetted perimeter to an equivalent pipe diameter. Each effect due to the addition of the inside

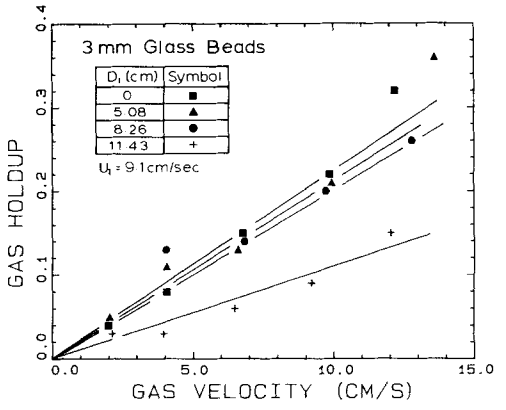

Figure 8. Overall gas holdup for 3 mm glass bead systems in dispersed bubble regime.
U_l = 9.1 cm/s

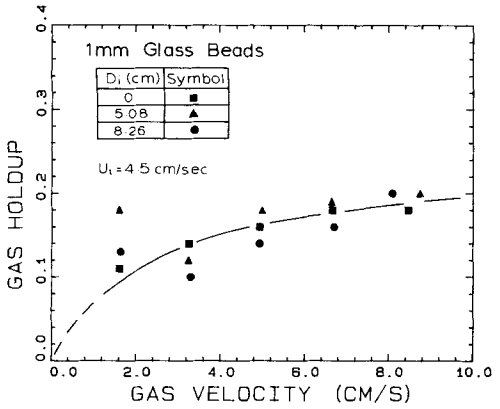

Figure 9. Overall gas holdup for 1 mm glass bead systems in dispersed bubble regime.
U_l = 4.5 cm/s

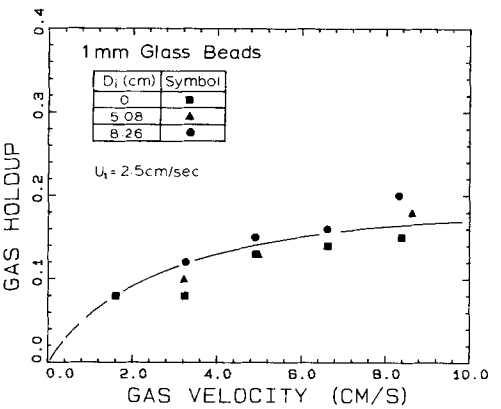

Figure 11. Overall gas holdup for 1 mm glass bead systems in coalesced bubble regime.
U_l = 2.5 cm/s

column implicitly reflects the increase, or lack of increase, in bubble size.

The change in transition velocity with D_h is shown in Figure 12. For both 1 mm and 3 mm particle systems, the transition velocity decreases almost linearly with D_h. This behavior indicates that the inside column promotes bubble coalescence in the bed.

Interpreting the experimental gas holdup data in terms of a relative bubble rise velocity adds insight into the effects of the inside column. Chern et al. (1984) adapted the Nicklin theory for two-phase bubble flow to three-phase systems. The resulting equation relates the gas holdup to a relative bubble velocity:

$$\frac{U_g}{\epsilon_g} = \frac{U_l}{\epsilon} + \frac{U_g}{\epsilon} + U_{br} \tag{5}$$

where ϵ is the bed voidage ($\epsilon_l + \epsilon_g$) and U_{br} is a velocity relative to a surface moving with velocity equal to the mean upward linear volume flux. Expressing the gas holdup data displayed in Figure 8, 9, and 10 in terms of U_{br} shows several trends. In both 3 mm particle and gas-liquid systems U_{br} depends weakly on the gas velocity and strongly on the size of the annulus region. In the 1 mm particle systems, however, U_{br} depends strongly on the gas velocity and weakly on the annulus size. The different trends result from the contrasting bubble behavior prevalent in each system.

U_{br} can be related to the bubble behavior through the bubble rise velocity. A gas phase material balance directly relates gas holdup to the bubble velocity

$$U_b = \frac{U_g}{\epsilon_g} \tag{6}$$

where U_b is the mean bubble velocity and ϵ_g is the overall gas holdup. Furthermore, the bubble velocity can also be expressed in terms of a slip velocity relative to the liquid velocity.

$$U_b = U_s + \frac{U_l}{\epsilon_l} \tag{7}$$

The slip velocity is usually expressed in terms of the infinite rise velocity of a single bubble modified to include any interaction with other bubbles (i.e., bubble swarms) or particles. Davidson and Harrison (1966) proposed that U_s be described by

$$U_s = \frac{U_\infty}{(1 - \epsilon_g)} \tag{8}$$

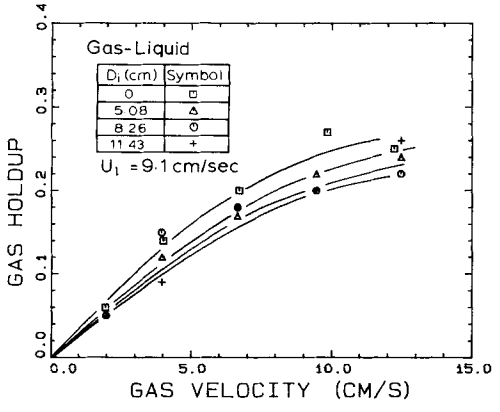

Figure 10. Overall gas holdup in gas-liquid system.
U_l = 9.1 cm/s

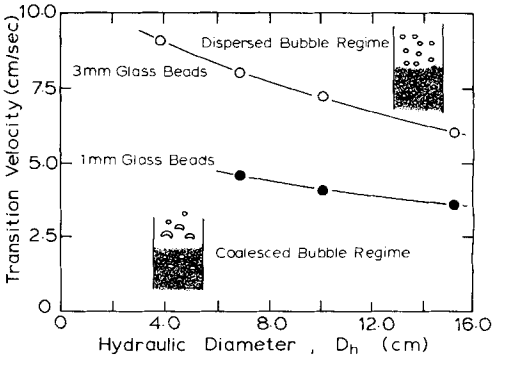

Figure 12. Change in flow regime transition velocity with hydraulic diameter.

Combining Eqs. 5, 6, 7, and 8 and subsequently solving for U_{br} in terms of U_∞ gives

$$U_{br} = U_\infty + \frac{\epsilon_s}{\epsilon}\left(\frac{\epsilon_g}{\epsilon_l} U_l - U_g\right) \tag{9}$$

This expression relates U_{br} to the fundamental bubble behavior through the infinite bubble rise velocity.

The infinite rise velocity, for large bubbles in systems having negligible viscosity and surface tension effects, can be determined through the Davies-Taylor relationship

$$U_\infty = \alpha(gD_b)^\beta \tag{10}$$

where α and β are constants. Substituting for U_∞ in Eq. 9 gives

$$U_{br} = \alpha(gD_b)^\beta + \frac{\epsilon_s}{\epsilon}\left(\frac{\epsilon_g}{\epsilon_l} U_l - U_g\right) \tag{11}$$

The behavior of U_{br} reflects the bubble size behavior directly for conditions in which the second term of Eq. 11 is insignificant. The conditions employed in experiments in the dispersed bubble regime fit in this category.

In the dispersed bubble regime, bubbles found in the 3 mm particle systems were small compared with those found in 1 mm particle systems. Since the rise velocity of a bubble depends on its size, U_{br} should show different behavior for the two systems. The change in the mean relative bubble rise velocity with D_h is shown in Figure 13. Two distinct trends are evident. In 3 mm particle systems U_{br} decreases dramatically with D_h, while in 1 mm particle systems U_{br} depends weakly on D_h. Bubble size measurements indicate that the presence of an inside column increases the bubble size over that found without an inside column. In small bubble systems this size increase is significant and is reflected in a corresponding increase in U_{br}. In large bubble systems the increase in bubble size is insignificant; consequently, the corresponding increase in U_{br} is also insignificant.

The experimental evidence clearly indicates that an annular fluidized bed behaves differently than a conventional fluidized bed of equal outside column diameter. This difference occurs in both the regime transition and holdup behavior. Since the presence of an inside column effectively reduces the cross-sectional area of the bed, it is interesting to note how a corresponding reduction in cross-sectional area through using a smaller diameter outside column affects the hydrodynamics. Yamashita (1983) determined gas holdup in the fluidization of a mixture of 3 mm and 4 mm glass beads within a 10.2 cm column. His data suggested that little difference occurred between the gas holdup in this binary mixture and that for 3 mm glass beads only. A comparison of Yamashita's data from a 10.2 cm column with the data acquired in the 15.2 cm column system used in this study is shown in Figure 14. The annular system with an 8.3 cm inside column has a D_h of 10.2 cm; this D_h is equivalent to that of Yamashita's system. Comparing the data between these two systems shows differences: at low gas velocities the behavior is similar, while at high gas velocities the gas holdup in the annular system is larger. Consequently, the hydraulic diameter proves inadequate when comparing systems with different outside column diameters.

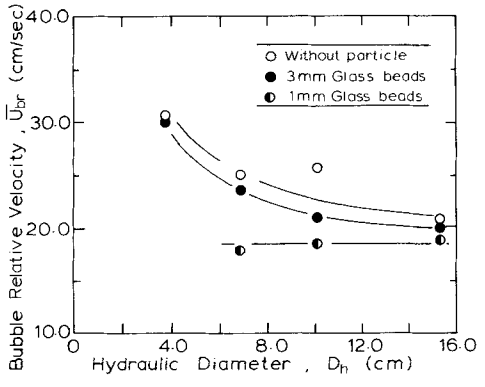

Figure 13. Effect of hydraulic diameter on relative bubble velocity.

Information about the column diameter effect on the bed hydrodynamics available in the literature is limited. Begovich and Watson (1978) presented a correlation derived solely from a statistical analysis of numerous data. According to their correlation, assuming all other parameters are constant, the gas holdup will increase with a decrease in column diameter. However, this suggested behavior incorrectly reflects the observed behavior presented in Figure 13. To be accurate, general correlations of holdup behavior that include column diameter effects must also consider the particle size effects, and consequently the bubble behavior of the system.

Application of the results presented in this study to industrial situations must involve careful consideration of the inside to outside column diameter ratio, the annulus thickness, and the properties of both gas and liquid phases under operating conditions.

Concluding Remarks

The experimental results show significant changes in the hydrodynamic behavior of annular systems over conventional systems. The liquid velocity of transition from the coalesced bubble regime to the dispersed bubble regime increases in both systems of 3 mm and 1 mm glass beads. The mean bubble size is larger in annular systems than in a nonannular system of equal outside column diameter. This behavior suggests an increased tendency for bubble coalescence in annular systems. For the fluidization of 3 mm glass beads, where the bubble sizes are relatively small, the increased tendency to coalesce produces sig-

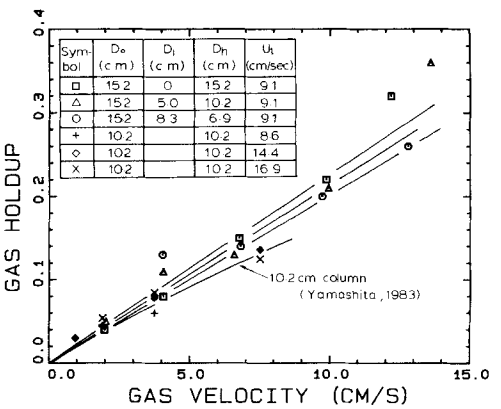

Figure 14. Comparison of gas holdup data obtained in fluidized beds having different outside diameters.

nificant changes in the hydrodynamic behavior. However, for the fluidization of 1 mm glass beads, where the bubble sizes are relatively large, the resulting increase in coalescence produces insignificant changes. Each of these phenomena is a manifestation of the bubble behavior.

The data on gas and solid holdups show small variations with annulus size when compared under equivalent flow regime situations. However, changes in regime transition behavior in annular systems cause significant variations in the holdup since the systems are in different flow regimes under the same gas and liquid velocities. For all cases studied, the effect of the inside column is small at low gas flow rates.

Acknowledgment

The National Science Foundation supported this work through Grant No. CPE-8219160.

Notation

A = bed cross-sectional area, cm^2
D_b = bubble diameter, cm
D_h = hydraulic diameter, cm
D_i = inside column diameter, cm
D_o = outside column diameter, cm
g = acceleration of gravity, cm/s^2
H = bed height, cm
P = pressure, cm H_2O
R = probability density
U_b = bubble velocity, cm/s
U_{br} = relative bubble velocity, cm/s
U_g = gas velocity, cm/s
U_l = liquid velocity, cm/s
U_s = slip velocity, cm/s
U_∞ = infinite rise velocity of a single bubble, cm/s
W = weight of particles in bed, g
Z = axial distance, cm

Greek letters

α = constant in Davies-Taylor relationship, cm/s
β = exponent in Davies-Taylor relationship
ϵ = bed voidage = $1 - \epsilon_s$
ϵ_g = gas holdup
ϵ_l = liquid holdup
ϵ_s = solids holdup
ρ_g = gas density, g/cm^3
ρ_l = liquid density, g/cm^3
ρ_s = particle density, g/cm^3
ξ = dimensionless bubble diameter

Literature cited

Akita, K., and Yoshida, F., "Bubble Size, Interfacial Area, and Liquid-Phase Mass Transfer Coefficient in Bubble Columns," *Ind. Eng. Chem. Process Des. Dev.* **13,** 84 (1974).

Begovich, J. M., and J. S. Watson, "Hydrodynamic Characteristics of Three-Phase Fluidization," *Fluidization,* J. F. Davidson and D. L. Keairns, eds., Cambridge Univ Press, 190 (1978).

Chern, S. H., L.-S. Fan and K. Muroyama, "Hydrodynamics of Cocurrent Gas-Liquid-Solid Semifluidization with a Liquid as the Continuous Phase," *AIChE J.,* **30,** 228 (1984).

Dakshinamurty P., K. Veerabhadra Rao, R. V. Subbaraju, and V. Subrahmanvam, "Bed Porosities in Gas-Liquid Fluidization," *Ind. Eng. Chem. Process Des. Dev.,* **11,** 318 (1972).

Davidson, J. F., and D. Harrison, "The Behavior of a Continuously Bubbling Fluidized Bed," *Chem. Eng. Sci.,* **21,** 731 (1966).

Eccles, R. M., and G. R. De Vax, "Current Status of H-Coal Commercialization," *Eng. Prog.* **77,** 80 (1981).

Fan, L.-S., A. Matsuura, and S. H. Chern, "Hydrodynamic Characteristics of a Gas-Liquid-Solid Fluidized Bed Containing a Binary Mixture of Particles," *AIChE J.,* **31,** 180 (1985).

Fan, L.-S., S. Satija, and K. Wisecarver, "Pressure Fluctuation Measurements and Flow Regime Transitions in Gas-Liquid-Solid Fluidized Beds," *AIChE J.,* **32,** 338 (1986).

Hirata, A., Y. Hosaka, H. Mukai, and M. Nara, "Biological Treatment of Phenolic Wastewater in a Three-Phase Fluidized Bed 1: Control of Biofilms by Mechanical Stirring," *Water Purification Liquid Wastewater Treatment* (Japan), **23,** 15 (1982).

Johnson, N. R., and A. M. Rapp, "H-Oil and Hy-C Eliminate Fuel Oils," *Hydr. Proc.,* **43,** 165 (1964).

Matsuura, A., and L.-S. Fan, "Distribution of Bubble Properties in a Gas-Liquid-Solid Fluidized Bed," *AIChE J.,* **30,** 894 (1984).

Michelsen, M. L., and K. Ostergaard, "Holdup and Fluid Mixing in a Gas-Liquid-Solid Fluidized Bed," *Chem. Eng. J.,* **1,** 37 (1970).

Muroyama, K., and L.-S. Fan, "Fundamentals of Gas-Liquid-Solid Fluidization," *AIChE J.,* **31,** 1 (1985).

Ramamurthy, K., and K. Subbarju, "Bed Expansion Characteristics of Annular Liquid-Solid Fluidized Beds," *Ind. Eng. Chem. Process Des. Dev.,* **12,** 87 (1973).

Van Driesen, R. P., and N. C. Stewart, "How Cities Services H-Oil Unit Is Performing," *Oil Gas J.,* 100 (May 18, 1964).

Wallis, G. B., *One-Dimensional Two-Phase Flow,* McGraw-Hill New York, 291 (1969).

Yamashita, T., "Solids Intermixing in a Gas-Liquid-Solid Fluidized Bed Containing a Binary Mixture of Particles," M. S. Thesis, Ohio State Univ. (1983).

Manuscript received Feb. 21, 1986, and revision received July 15, 1986.